nature physics

ARTICLES

PUBLISHED ONLINE: 29 JUNE 2014 | DOI: 10.1038/NPHYS3013

Demonstration of magnetically activated and guided isotope separation

Thomas R. Mazur, Bruce Klappauf and Mark G. Raizen*

Enriched isotopes are widely used in medicine, basic science and energy production, and the need will only grow in the future. The main method for enriching stable isotopes today, the calutron, dates back over eighty years and has an uncertain future, creating an urgent need, especially in nuclear medicine. We report here the experimental realization of a general and efficient method for isotope separation that presents a viable alternative to the calutron. Combining optical pumping and a unique magnet geometry, we observe substantial depletion of Li-6 throughput in a lithium atomic beam produced by an evaporation source over a range of flux. These results demonstrate the viability of our method to yield large degrees of enrichment in a manner that is amenable to industrial scale-up and the production of commercially relevant quantities.

In 1930, Ernest Lawrence invented the cyclotron, which later developed into a general method for isotope separation based on ionization of atoms with electrons, and separation by the charge-to-mass ratio[1]. The first such machine, the calutron, invented for the Manhattan Project in World War II, was later realized as a general-purpose apparatus that could provide small quantities of most stable isotopes in the periodic table[2,3]. These enriched stable isotopes are generally converted to radio-isotopes in nuclear reactors or accelerators[4]. The United States, however, decommissioned the last of its calutrons in 1998 owing to high maintenance and operating costs[5]. Today, the world depends heavily on the calutron programme in Russia for many stable isotopes, but even those machines are over sixty years old[6]. Despite years of effort, no single method has emerged as a viable general alternative to the calutron, in terms of degree of enrichment, scalability and efficiency[7,8]. In response to this challenge, we proposed magnetically activated and guided isotope separation (MAGIS; refs 9,10). In this article, we present the first experimental demonstration of MAGIS that implies high levels of enrichment in a scalable and efficient fashion.

Three criteria for any effective isotope separation technique include the ability to achieve purity that meets or exceeds market demand, scale an apparatus to the production of commercially relevant quantities, and operate efficiently, which entails maximizing the ratio between enriched material and feedstock, requiring sustainable power consumption, and being applicable to multiple elements. Defining absolute standards for these criteria is challenging both as a result of variations in physical properties and also differences in applications and the concomitant value of various isotopes. For reference, a figure-of-merit is that a single calutron can process 0.1 mol multiplied by the relative abundance of an isotope per day of operation[11]. The attainable purity from a single pass through a calutron varies substantially. Extensive tables provide degrees of enrichment for isotopes processed by calutrons at Oak Ridge National Laboratory (ORNL), with enrichment factors for many isotopes ranging between 100 and 1,000 (ref. 12). Note that the enrichment factor is defined by $[(N_1/(1\text{-}N_1)]/[N_0/(1\text{-}N_0)]$ where N_1 and N_0 denote the relative abundances of the isotope after and before enrichment. A key feature of the calutron is that all isotopes of a given element can be simultaneously enriched. Although ORNL ultimately used calutrons to enrich over 235 isotopes of 56 elements, the energy input for one machine—largely contributing to maintaining the ∼1 T static magnetic field—was large. In some cases, the energy input exceeded 1 TJ for enriching just a gram of material[13]. Although it is beyond the scope of this work to address alternative separation techniques individually, none have yet achieved the general applicability and implementation necessary to supplant the calutron[8].

Our approach relies on optical pumping, first described by Kastler in 1950 (ref. 14), to magnetically polarize atoms of a targeted isotope, followed by a magnetic field gradient that efficiently guides atoms of a desired isotope to a collection plane. A key aspect of our approach is that optical pumping requires that each atom of a targeted isotope scatter only a few photons on average to change its internal state. As a result, laser powers feasibly produced by inexpensive semiconductor lasers should enable many moles of material to be enriched per year[10]. The subsequent two-dimensional magnetic field gradient—produced in this demonstration using rare-earth magnets—then accomplishes enrichment of a desired isotope. The design of the magnet array yields a competitive ratio between enriched material and feedstock that depends only on source temperature. By extending the height of this field gradient and adding additional arrays about the atomic source, the solid angle subtended by the collection plane to the source can be engineered to be several steradians.

Other magneto-optic systems have combined similar principles toward isotope separation[15–17]. These systems, however, provided little enrichment, with no apparent means of scaling production toward meaningful quantities or continuous use. Magneto-optic traps, for instance, offer no opportunities for macroscopic production, separating fg s^{-1} generally[17]. Other work derived from a thermal beam demonstrated a change in the isotopic ratio of lithium by a substantially smaller amount than that reported here and achieved significantly lower throughput in a commercially unfeasible magnetic configuration[15].

Although we apply our approach towards production of enriched Li-7 (HDLi, for lithium highly depleted of Li-6), application of our method to a given element requires just a suitable magnetic state accessible by optical pumping and also a low vapour pressure at the apparatus temperature. Lithium, with stable isotopes Li-6

Center for Nonlinear Dynamics and Department of Physics, The University of Texas at Austin, Austin, Texas 78712, USA.
*e-mail: raizen@physics.utexas.edu

(7.5% abundance) and Li-7 (92.5% abundance), is an especially relevant test case, however, owing to the importance of HDLi for the nuclear power industry. HDLi is used today in nuclear reactor cooling water, and is required to have a purity of over 99.9% (ref. 18). Future reactor designs using molten salt will require much larger quantities of HDLi, and at even higher purity[19]. The current method for production of HDLi is the column-exchange method, which was shut down in the United States in 1963 after tons of mercury were released into the environment[20]. The phase-out of this method worldwide seems inevitable, creating an urgent need for the development of an alternative method[21].

Figure 1 outlines our three-stage process—evaporation, magnetic activation through optical pumping, and magnetic separation—applied to enriching Li-7 for this demonstration. The source is a stainless steel reservoir that we typically operate between 550 and 750 °C. We load the source with either natural lithium or enriched Li-6, with the latter enabling higher sensitivity to the suppression of Li-6 throughput with certain detectors. We constrain the source area using a narrow vertical aperture just after the source exit to provide a well-defined initial position for atomic trajectories, mainly for comparing results to numerical simulations. Both lithium isotopes initially have thermal distributions of atomic states such that in a sufficiently large magnetic field (>40 G), roughly half the population of each isotope will be attracted to high magnetic field (high-field seekers) and half repelled by high magnetic field (low-field seekers)[22].

In the optical pumping section, a broad 671 nm laser beam, shown as a red arrow in Fig. 1, transversely illuminates the atomic beam. The laser prepares a large fraction of Li-6 atoms in the high-field-seeking $F = \frac{1}{2}$ ground state. As the isotope shift between Li-6 and Li-7 is sufficient for Li-7 atoms to remain unaffected, the only atoms able to be deflected after optical pumping are low-field-seeking Li-7 atoms, thus providing a mechanism for separation of Li-7 (ref. 23). Using a simple semiconductor laser system, yielding at most 150 mW of usable power, we observe little variation in purity over a range of laser power.

Following the optical pumping section, a large chamber, connected to the pumping region with a flexible bellows, contains the magnets. The ~3.8 cm tall magnet array, exaggerated in Fig. 1 as the blue line, consists of 480 neodymium–iron–boron magnets arranged in a Halbach configuration that is 1.5 m long and bent over its length by 20 mrad in order to facilitate the blocking of atoms too fast to be deflected. An aperture, 1.5 cm wide by 2 cm high, is attached to the front of the magnet array to obstruct line-of-sight from the slit defining the atomic source to the collection region beyond the slightly curved magnet barrier, as further illustrated in Fig. 2a.

We dynamically monitor purity and flux using an array of detectors beyond the magnets. A commercial residual gas analyser (RGA) samples a slice of flux beyond the magnets, yielding isotopic abundances. Owing to limited resolution and signal-to-noise, we use the RGA for measuring suppression of Li-6 when loading the source with enriched Li-6. We measure Li-6 suppression when using natural lithium in the source by diverting a fraction of laser power to beyond the magnets and imaging laser-induced fluorescence onto a CCD camera. Translating a surface ionization detector (or wire detector), consisting of a 800 μm wide by 70 mm tall rhenium ribbon[24], across the collection plane we can measure the spatial profile of the flux. Supplementing these traces with measurements made with a quartz crystal thickness monitor that also translates across the collection plane, we extract a quantitative determination of the throughput. Measuring the flux in the optical pumping region using the thickness monitor, we determine the flux corresponding to a nominal temperature then ultimately obtain a quantitative estimate for the efficiency of the magnetic guide by comparison to the throughput measured beyond the magnets.

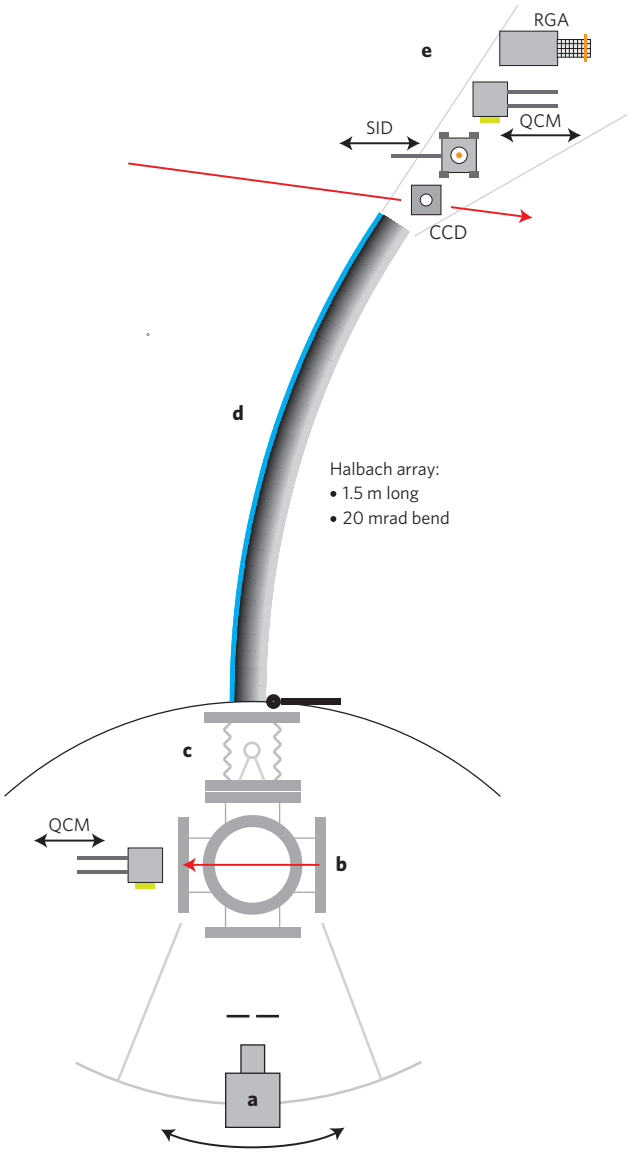

Figure 1 | Schematic top-down view of apparatus used for lithium separation. Atoms evaporated from the source (**a**) pass through a narrow aperture before entering the optical pumping region (**b**). The beam line leading up to the magnet array (**d**) pivots about a bellows (**c**) that interfaces the front end of the apparatus to the magnets. Beyond the magnets we use four detectors (**e**) for dynamically characterizing the throughput. Fluorescence imaged onto a charge-coupled device (CCD) and an residual gas analyser (RGA) gives isotopic abundances, while a wire detector (surface ionization detector (SID)) and thickness monitor (QCM) give throughput estimates. The thickness monitor can be moved to the optical pumping region to estimate the flux entering the magnetic guide.

Before making any purity or flux measurements, we optimize the incidence angle of the thermal beam onto the magnet array by rotating the source and optical pumping sections about the bellows interfacing to the guide chamber, as shown schematically in Fig. 2a. Moving the source too far to the left (blue wire detector measurement in Fig. 2b) grants line-of-sight to the collection area and reduces purity. In contrast, translating the source too far to the right (orange trace in Fig. 2b) chokes off throughput as the far edge of the aperture progressively obstructs more of the magnet surface, and velocity components perpendicular to the face of the array increase, decreasing the maximum velocity for trajectories that can be reflected. The optimal position for the source (green trace in

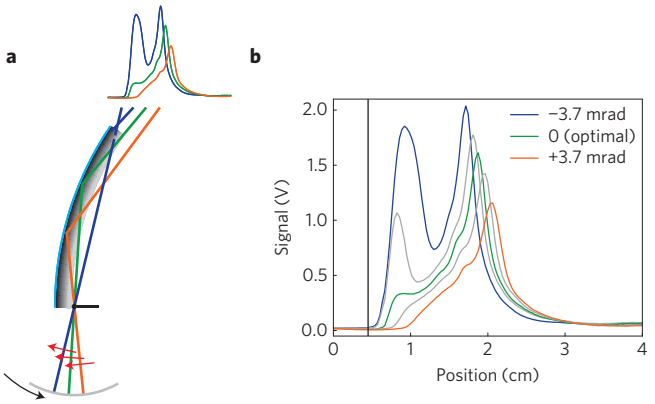

Figure 2 | Effect of source position on the profile of lithium throughput. **a**, Translating the source closer to line-of-sight past the magnets yields higher throughput (orange then green), however moving too far (blue) grants line-of-sight past the magnets, thus yielding a second observed peak in the throughput corresponding to undeflected atoms. **b**, Actual wire scan signals for different source positions (coloured traces corresponding to representative cases in **a**). Positions granting line-of-sight show a cutoff at roughly the same location corresponding to the shadow of the last magnet (vertical black line). Moving away from line-of-sight instead shows an entrance aperture shadow moving to the right in addition to reduced peak heights.

Fig. 2b) is the closest attainable position to line-of-sight that does not actually grant sight. In this location, the apparatus should yield complete suppression of Li-6, assuming perfect optical pumping, while maximizing Li-7 throughput past the magnet barrier. Numerical simulation suggests that at a source temperature of 600 °C over 25% of the Li-7 distribution (50% of the low-field-seeking atoms) incident on the magnet barrier could reach the collection plane[10].

Maximizing Li-6 depletion requires that a variety of parameters, including laser power, frequency, linewidth, beam shape, incidence angle, height, polarization and quantization axis, be optimized. Figure 3a shows mass scans from the RGA that span masses 6 and 7 with the source loaded with enriched Li-6, indicating substantial depletion of Li-6. The figure compares the average of ten scans with (red) and without (blue) optical pumping after subtracting an averaged background scan (grey). These traces were recorded with our first-generation source, nominally operating at 550 °C (as indicated by the thermocouple). Taking the quotient of the integrals about the peaks of the two traces in Fig. 3a, we determine that Li-6 throughput is suppressed by a factor of 280 ± 70 whereas the Li-7 fraction remains unchanged. Extrapolating to natural lithium, starting with a Li-7 fraction of 92.5%, such depletion of Li-6 would yield a Li-7 purity of (99.97 ± 0.01)%. As shown in the Supplementary Information we readily suppress Li-6 throughput when running enriched Li-6 by a factor larger than 100 at source temperatures up to 600 °C (directly measuring the atomic flux in the pumping region using the thickness monitor) over a range of laser intensities. While the RGA measures flux at one position beyond the magnets, the wire traces in Fig. 4c confirm drastic Li-6 suppression across the entire collection plane.

Figure 3b shows measurements of Li-6 suppression obtained from fluorescence imaged onto a CCD (blue) and also atomic flux in the pumping region measured with the thickness monitor (green) as a function of temperature (up to 750 °C) with the source loaded with natural lithium. Depletion measurements correspond to the ratio of integrated pixel intensities of background-subtracted images without and with optical pumping. The dashed red line corresponds to the necessary Li-6 suppression for enrichment of Li-7 to 99.95%. Despite the reduction in depletion at the peak temperatures, probably owing to one of the systematic effects discussed in the Supplementary Information (ref. 25), the depletion factor remains at or above 100, and we expect to improve these figures as we further explore the parameter space for optical pumping.

To quantitatively estimate the throughput and efficiency of the guide, we first measured a response function for the thickness monitor by translating the 8.25 mm diameter sensor across a 1 mm wide slit positioned in the pumping region where the flux is uniform over an extended width. After removing the slit, we measured the mass deposition rate for various source temperatures, from which we extrapolated the flux entering the guide aperture based on the apparatus geometry. As illustrated in Fig. 4a, we then translated the thickness monitor across the collection plane just beyond the wire detector at various source temperatures. As discussed in more detail in the Supplementary Information, a data point for the thickness monitor corresponds to the convolution of the actual throughput over the sensor area with the measured response function. A wire detector trace yields an approximation for the shape of the actual throughput about the relevant point. By scaling the wire detector measurement to have the convolution yield the deposition rate obtained with the thickness monitor, we determine a calibration for the wire trace. We then can integrate this trace across the entire collection plane to estimate the absolute throughput.

Figure 4b shows thickness monitor measurements and calibrated wire traces for natural lithium at 650 and 700 °C source temperatures. At these temperatures, we estimate the absolute throughput to be $(7.2 \pm 0.9) \times 10^{11}$ and $(1.4 \pm 0.1) \times 10^{12}$ atoms s^{-1} mm^{-1} of collection plane height, respectively. Comparison against the estimated flux incident on the guide aperture (derived from measurements including those shown in Fig. 3b) gives efficiencies for the guide at these temperatures of 0.26 ± 0.04 and 0.21 ± 0.03, respectively. Using enriched Li-6 with the source at 600 °C, as shown in Fig. 4c, we can similarly estimate the throughput to be $(5.4 \pm 0.7) \times 10^{11}$ atoms s^{-1} mm^{-1} of collection plane height. Note that the black trace in Fig. 3c shows the resulting profile from a numerical simulation. We used the line-of-sight threshold, evident in Fig. 2b, to impose a horizontal offset to overlay the traces. We then scaled the amplitude to obtain a reasonable match. We attribute the discrepancy between simulated and actual throughput to sensitivity to the exact arrangement of the magnet array.

These quantitative measurements can be geometrically scaled based on the number and size of the guides. As the magnet array is two-dimensional, scaling the throughput without sacrificing purity proceeds by extending the height of the arrays and arranging additional arrays about the source. Per vertical metre of guide entrance, the measured throughputs above for natural lithium scale linearly to 0.8 ± 0.1 and 1.6 ± 0.2 g yr^{-1} of continuous operation. Thus, 50 guides each 3 m tall arranged about a source operated at 700 °C could produce in excess of 200 g yr^{-1} of enriched Li-7, on par with the figure given earlier for the calutron but without the massive energy input needed for maintaining its magnetic field. Engineering guides to maximize the solid angle subtended by the collection plane will enable even larger throughputs. On a commercial apparatus, the efficiency per guide gives an upper limit for overall efficiency, as not all material evaporated from the source will reach a guide. By engineering the apparatus such that the guide entrances subtend a large fraction of the solid angle to the source, the overall efficiency should be a large fraction of the estimates given here. Using a larger source area will yield a comparable flux at lower source temperatures, where the guide efficiency is better.

To elaborate on energy consumption, figures-of-merit for calutron performance suggest that enriching 1 g of Li-7 should require over 10 GJ of energy input just for maintaining the magnetic field[12,13]. Moreover, close to 200 MJ should be needed for accelerating ions produced in the source. In contrast, a resistively heated source—like that used for the throughput measurements presented in Fig. 4—would consume close to 40 MJ while yielding

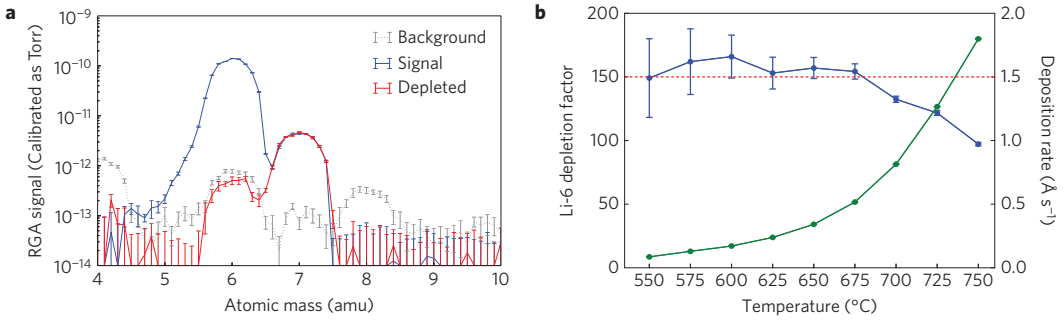

Figure 3 | Isotope-selective measurements. a, Residual gas analyser (RGA) scan from mass 4 to 10 amu with the source at 550 °C while using enriched Li-6. The blue trace shows the background subtracted average of the lithium reaching the RGA without optical pumping. The red trace shows the background subtracted average of the same signal when the optical pumping laser is applied. We see depletion of Li-6 by $(3.6 \pm 0.9) \times 10^{-3}$ with no effect on Li-7 throughput. The light grey trace was the RGA signal with the lithium beam blocked, showing that we were depleting to nearly the limit of our detector. **b**, Li-6 depletion (blue) measured via fluorescence as a function of source temperature while using natural lithium. Thickness monitor measurements (green) give atomic flux in the pumping region at each temperature. The dashed red line shows the threshold for achieving Li-7 enrichment to 99.95%. Error bars show standard deviations from the mean.

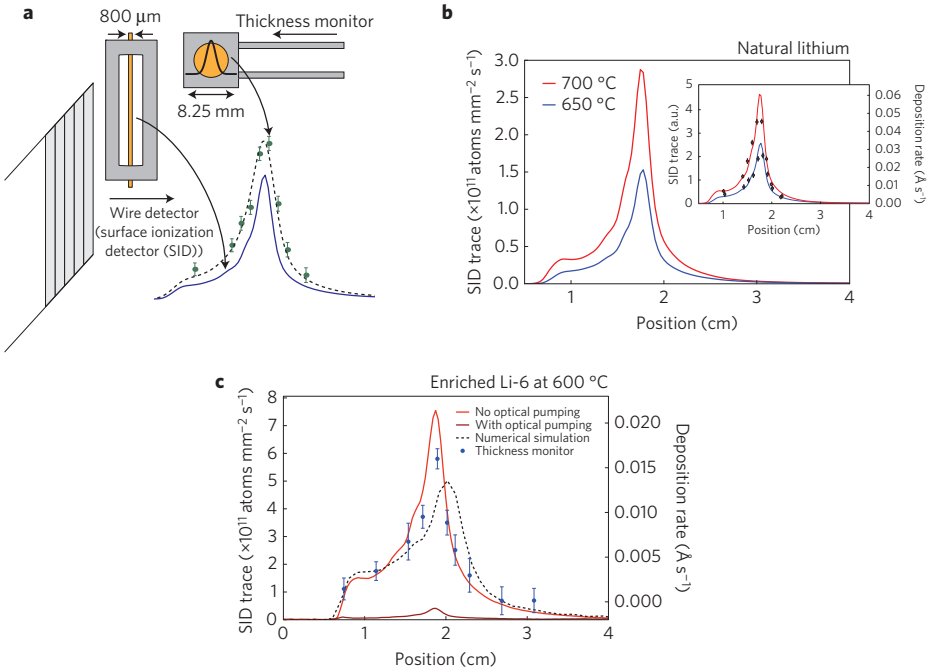

Figure 4 | Throughput and efficiency measurements. a, Schematic overview of the procedure for estimating throughput. We first measure a response function for the thickness monitor (black trace overlaying the thickness monitor) with the thickness monitor in the pumping region. We then identify a calibration factor for a wire trace (blue) that reasonably approximates the thickness monitor data (dashed black curve is calculated and green points are data) when taking convolutions with the response function over the sensor area. With this factor we can integrate the wire trace to get a throughput number. **b**, Calibrated wire traces at 650 °C (blue) and 700 °C (red) when using natural lithium in the source. The inset shows the wire traces and thickness monitor deposition rates that give the calibration. As expected, the efficiency worsens at higher temperature whereas the throughput increases. The deposition rates measured in the pumping region at these temperatures are 0.341 ± 0.001 Å s^{-1} and 0.814 ± 0.003 Å s^{-1}, respectively. **c**, Wire traces (red and dark red) and thickness monitor deposition rates (blue) at 600 °C when using enriched Li-6 in the source. Comparison of wire traces with (dark red) and without (red) the optical pumping light confirm drastic suppression of Li-6 over the entire collection plane. A numerical simulation for 800 K (dashed black) shows qualitative agreement with the experiment. The exact shape of the throughput should be highly sensitive to the exact geometry of the magnet array. We similarly can estimate throughput using the thickness monitor deposition rates. Error bars show standard deviations from the mean.

1 g of Li-7 in a scaled apparatus like that described above. Although this source worked effectively for characterizing throughput in this proof-of-principle apparatus, various simple design changes should reduce its energy consumption drastically. The remaining non-shared energy expense for MAGIS is that required for operating the lasers for optical pumping. With low laser powers (< 1 W) generally being sufficient for enriching many moles of material, this cost should not exceed a MJ per gram of Li-7 (ref. 10).

Although here we have presented an experimental demonstration of MAGIS applied to lithium, we also have identified 129 other isotopes (Supplementary Information) as candidates for this process. We have found long-lived magnetic states for each of these isotopes with optical pumping wavelengths that can be readily produced using commercial solid state laser systems. Moreover, the magnetic reflection is mass-independent, and in fact will work better for certain heavier isotopes with lower

operating temperatures and guided states with higher magnetic moments. Proliferation concerns related to the actinides have been addressed elsewhere[26]. Because of this broad applicability, combined with attainable enrichment, throughput and efficiency, we believe we can mitigate the loss of isotope production due to the shutdown of the calutrons. Therefore, we believe that MAGIS will make possible new areas of research and development by providing an economical source for a wide range of stable isotopes. Future work will focus on tailoring and scaling the principles of MAGIS for enriching larger quantities of material at higher purities. Points of emphasis towards these efforts will be improving the efficiency of the atomic source, investigating alternative means for realizing magnet arrays, and reaching higher degrees of enrichment.

Methods

Although the source geometry varied for certain measurement sets (see Supplementary Information for more detail), we typically load the source with tens of grams of material at a time. Using feedback control, we maintain the source temperature to within $\pm 1\,^{\circ}\mathrm{C}$, as measured by a thermocouple. Atoms exit the source reservoir through a 1 cm diameter tube. At our peak operating temperatures, we heat this tube to at least 50 °C beyond the reservoir temperature to prevent clogging. We likewise heat the aperture directly in front of the source to beyond the source operating temperature to ensure that material does not condense and obstruct the opening.

We perform optical pumping on the transition between the $^2S_{1/2}$ ($F=3/2$) ground state and the $^2P_{1/2}$ ($F'=3/2$) excited state. After a few transitions, a Li-6 atom will decay to the $F=1/2$ ground state, which is high-field-seeking in fields above 40 gauss. The splitting between the $F=1/2$ and $3/2$ ground states is sufficient to prevent the laser from appreciably pumping atoms out of the $F=1/2$ ground state. We double-pass the light through an electro-optic modulator driven at 6 MHz to effectively broaden the laser bandwidth to as much as 50 MHz. We produce the light using a tapered amplifier seeded by a grating-stabilized external-cavity diode laser. We stabilize this laser via a frequency-offset lock using another laser that is referenced to a line on the Li-6 spectrum using saturation absorption spectroscopy.

In a Halbach array, the magnetization direction of each magnet (oriented through the magnet thickness) is rotated by 90° about the magnet length between adjacent magnets. In this configuration, the magnetic field is amplified to close to 1 T (confirmed via measurements with a gaussmeter) on one face of the magnets while being nearly completely attenuated on the opposite face. A 0.05 mm stainless steel shim covers the magnet surface to prevent lithium from contaminating the magnets. The magnet array and detectors occupy an aluminium chamber that interfaces to the source and optical pumping regions via a large bellows. The beam line leading up to the bellows (including all optics) pivots about the aperture at the front of the magnet array. The entire apparatus is maintained under vacuum at pressures below 1×10^{-7} Torr.

A stainless steel cylinder (with an opening for sampling the atomic beam) surrounds the rhenium ribbon for the surface ionization detector. With a small bias voltage on this cylinder, we measure an ion current through a low-noise transimpedance amplifier as we translate the detector across the collection plane. A stepper motor actuates motion across the collection plane, and at every point we average the amplifier output over a large number of measurements.

The RGA consists of an ionization source (sampling the collection plane) followed by a quadrupole mass filter and electron multiplier. In contrast to the fluorescence measurements, the RGA allows us to confirm that Li-7 throughput is not affected by the optical pumping. Although we positioned the RGA close to where the throughput is maximal, the RGA cannot translate. We measure Li-6 suppression via fluorescence when using natural lithium in the source due to the mass 7 amu signal on the RGA 'bleeding' into the mass 6 amu signal, complicating data analysis. We position a large diameter lens as close as possible to the fluorescence beyond the magnets for imaging. We choose the focal length of this lens to roughly achieve one-to-one imaging of the fluorescence onto a cooled CCD sensor. To maximize fluorescence, the fluorescence beam double-passes an acousto-optic modulator to generate an additional beam 228 MHz detuned from the optical pumping beam. The resulting beams then pump Li-6 atoms out of both the $F=1/2$ and $F=3/2$ ground states.

Received 3 March 2014; accepted 3 June 2014;
published online 29 June 2014

References

1. Lawrence, E. & Livingston, M. The production of high speed light ions without the use of high voltages. *Phys. Rev.* **40,** 19–35 (1932).
2. Love, L. O. Electromagnetic separation of isotopes at Oak Ridge: An informal account of history, techniques, and accomplishments. *Science* **182,** 343–352 (1973).
3. Yergey, A. L. & Yergey, A. K. Preparative scale mass spectrometry: A brief history of the calutron. *J. Am. Soc. Mass Spectrom.* **8,** 943–953 (1997).
4. Adelstein, S. J. & Manning, F. J. *Isotopes for Medicine and the Life Sciences* (National Academies, 1995).
5. Brown, D. & Harrison, S. *Isotope Production and Applications in the 21st Century* 123–128 (World Scientific Publishing Company, 2000).
6. Rivard, M. J. *et al.* The US National Isotope Program: Current status and strategy for future success. *Appl. Radiat. Isotopes* **63,** 157–178 (2005).
7. Norenberg, J. *et al. Workshop on the Nation's Need for Isotopes: Present and Future.* DOE/SC-0107 (US Department of Energy, 2008).
8. Isotopes for the Nation's Future: A long range plan. Nuclear Science Advisory Committee: http://science.energy.gov/~/media/np/nsac/pdf/docs/nsaci_ii_report.pdf (2009).
9. Jerkins, M., Chavez, I., Even, U. & Raizen, M. G. Efficient isotope separation by single-photon atomic sorting. *Phys. Rev. A* **82,** 033414 (2010).
10. Raizen, M. G. & Klappauf, B. Magnetically activated and guided isotope separation. *New J. Phys.* **14,** 023059 (2012).
11. Newman, E. *Separated Isotopes: Vital Tools for Science and Medicine,* 45–80 (National Academy, 1982).
12. Bell, W. & Tracy, J. *Stable Isotope Separation in Calutrons: Forty Years of Production and Distribution.* ORNL/TM–10356 (Oak Ridge National Laboratory, 1987).
13. Terry, J. W. *Alternative Isotope Enrichment Processes.* CONF–8309127–1 (Oak Ridge National Laboratory, 1983).
14. Kastler, A. Quelques suggestions concernant la production optique et la détection optique d'une inégalité de population des niveaux de quantifigation spatiale des atomes. Application à l'expérience de Stern et Gerlach et à la résonance magnétique. *J. Physique Radium* **11,** 255–265 (1950).
15. Xiwen, Z., Guilong, H., Ganghua, M. & Delin, Y. Laser isotope enrichment of lithium by magnetic deflection of a polarized atomic beam. *J. Phys. B* **25,** 3307–3314 (1992).
16. Van Wijngaarden, W. & Li, J. Laser isotope separation of barium using an inhomogeneous magnetic field. *Phys. Rev. A* **49,** 1158–1164 (1994).
17. Noh, H. R., Kim, J. O., Nam, D. S. & Jhe, W. Isotope separation in a magneto-optical trap. *Rev. Sci. Instrum.* **67,** 1431–1433 (1996).
18. Kok, K. D. *Nuclear Engineering Handbook* (Mechanical Engineering Series, Taylor & Francis, 2010).
19. LeBlanc, D. Molten salt reactors: A new beginning for an old idea. *Nucl. Eng. Des.* **240,** 1644–1656 (2010).
20. Bruce, G. M., Flack, S. M., Mongan, T. R. & Widner, T. E. *Mercury Releases from Lithium Enrichment at the Oak Ridge Y-12 Plant: A Reconstruction of Historical Releases and Off-site Doses and Health Risks*. Reports of the Oak Ridge Dose Reconstruction (Tennessee Department of Health, 1999).
21. *Managing Critical Isotopes: Stewardship of Lithium-7 is Needed to Ensure a Stable Supply*. GAO-13-716 (United States Government Accountability Office, 2013).
22. Kusch, P., Millman, S. & Rabi, I. The radiofrequency spectra of atoms hyperfine structure and Zeeman effect in the ground state of Li^6, Li^7, K^{39} and K^{41}. *Phys. Rev.* **57,** 765–780 (1940).
23. Noble, G., Schultz, B., Ming, H. & van Wijngaarden, W. Isotope shifts and fine structures of ^{6,7}LiD lines and determination of the relative nuclear charge radius. *Phys. Rev. A* **74,** 012502 (2006).
24. Delhuille, R. *et al.* Optimization of a Langmuir–Taylor detector for lithium. *Rev. Sci. Instrum.* **73,** 2249–2258 (2002).
25. Gillot, J., Gauguet, A., Büchner, M. & Vigué, J. Optical pumping of a lithium atomic beam for atom interferometry. *Eur. Phys. J. D* **67,** 263 (2013).
26. The Risks and Benefits of Laser Isotope Separation Federation of American Scientists: http://www.fas.org/policy/debates/20120716/ (2012).

Acknowledgements

The authors would like to thank K. Melin for his contributions to the experiment.

Author contributions

T.R.M., B.K. and M.G.R. contributed equally to the experiment. All authors discussed the results and commented on the manuscript.

Additional information

Supplementary information is available in the online version of the paper. Reprints and permissions information is available online at www.nature.com/reprints. Correspondence and requests for materials should be addressed to M.G.R.

Competing financial interests

The authors declare no competing financial interests.